The PANDA Barrel DIRC

2016 JINST 11 C05013

(http://iopscience.iop.org/1748-0221/11/05/C05013)

Published by IOP Publishing for Sissa Medialab
Received: *March 15, 2016*
Accepted: *May 5, 2016*
Published: *May 13, 2016*

International Workshop on Fast Cherenkov Detectors - Photon detection, DIRC design and DAQ
November 11–13, 2015, Giessen, Germany

The PANDA Barrel DIRC

R. Dzhygadlo,[a] **C. Schwarz,**[a,1] **A. Belias,**[a] **A. Gerhardt,**[a] **K. Götzen,**[a] **G. Kalicy,**[a] **M. Krebs,**[a] **D. Lehmann,**[a] **F. Nerling,**[a] **M. Patsyuk,**[a] **K. Peters,**[a] **G. Schepers,**[a] **L. Schmitt,**[a] **J. Schwiening,**[a] **M. Traxler,**[a] **M. Zühlsdorf,**[a] **A. Britting,**[b] **W. Eyrich,**[b] **A. Lehmann,**[b] **M. Pfaffinger,**[b] **F. Uhlig,**[b] **M. Düren,**[c] **E. Etzelmüller,**[c] **K. Föhl,**[c] **A. Hayrapetyan,**[c] **B. Kröck,**[c] **O. Merle,**[c] **J. Rieke,**[c] **M. Schmidt,**[c] **E. Cowie,**[d] **T. Keri,**[d] **P. Achenbach,**[e] **M. Cardinali,**[e] **M. Hoek,**[e] **W. Lauth,**[e] **S. Schlimme,**[e] **C. Sfienti**[e] **and M. Thiel**[e]

[a] *GSI Helmholtzzentrum für Schwerionenforschung GmbH, Darmstadt, Germany*
[b] *Friedrich Alexander-University of Erlangen-Nuremberg, Erlangen, Germany*
[c] *II. Physikalisches Institut, Justus Liebig-University of Giessen, Giessen, Germany*
[d] *University of Glasgow, Glasgow, United Kingdom*
[e] *Institut für Kernphysik, Johannes Gutenberg-University of Mainz, Mainz, Germany*

E-mail: C.Schwarz@gsi.de

Abstract: The PANDA detector at the international accelerator Facility for Antiproton and Ion Research in Europe (FAIR) addresses fundamental questions of hadron physics. Experiments concerning charmonium spectroscopy, the search for hybrids and glueballs and the interaction of hidden and open charm particles with nucleons and nuclei will be performed with antiproton beams impinging on hydrogen or nuclear targets. Cooled beams allow the precision scan of resonances in formation experiments. The momentum range of the antiproton beam between 1.5 GeV/c and 15 GeV/c tests predictions by perturbation theory and will reveal deviations originating from strong QCD. An excellent hadronic particle identification will be accomplished by DIRC (Detection of Internally Reflected Cherenkov light) counters. The design for the barrel region is based on the successful BaBar DIRC with several key improvements, such as fast photon timing and a compact imaging region. DIRC designs based on different radiator geometries with several focusing options were studied in simulation. The performance of each design was characterized in terms of photon yield and single photon Cherenkov angle resolution. Selected design options were implemented in prototypes and tested with hadronic particle beams at GSI and CERN.

Keywords: Cherenkov detectors; Photon detectors for UV, visible and IR photons (vacuum)

[1] Corresponding author.

doi:10.1088/1748-0221/11/05/C05013

2016 JINST 11 C05013

Contents

1 Introduction

The PANDA[1] experiment [1] pursues a rich experimental physics program with a universal and hermetic detector capable of detecting charged and neutral particles with nearly 4π solid angle coverage and high resolution. Hidden-charm physics and the search for exotics require the detection of lepton pairs as well as good kaon identification and high efficiency for open-charm final states. Open-charm spectroscopy and electromagnetic reactions have similar demands. The decay of a charmed hadron releases rather high transversal momenta of up to $p_T = 1.5\,\mathrm{GeV/c}$ as compared to light and even strange meson decays. This leads to large opening angles of particles in the laboratory reference frame. Most of the channels of interest are expected to have very low cross sections, typically in the order of nb or pb. Due to the fact that the total antiproton-proton cross section is more than 40 mb in the energy regime of the PANDA measurements, a good background rejection power is mandatory. The particle identification (PID) requirements, as well as the PID systems covering the detection in forward direction for polar angles smaller than 22°, are described in ref. [2–4]. In this paper, the charged hadron PID for the barrel section of the target spectrometer is described. It covers the angular range of 22–140 degrees and needs to separate pions from kaons for momenta of up to 3.5 GeV/c with a separation power of at least 3 standard deviations (s.d.). The angular and momentum range of the Barrel DIRC acceptance is indicated in figure 1.

The PID has to operate within a solenoid with a strong magnetic field of $B \approx 2\,\mathrm{T}$ and at interaction rates up to 20 MHz. The electromagnetic calorimeter that surrounds the PID system imposes requirements like a small radius and a limited radiation length. These requirements can be met by a Ring Imaging Cherenkov Detector based on the DIRC principle [5]. Here, the radiator serves as a lightguide towards the photon detector. It consists of rectangular shaped bars or plates

[1] $\bar{\mathrm{P}}$ANDA : antiProton ANnihilation at DArmstadt

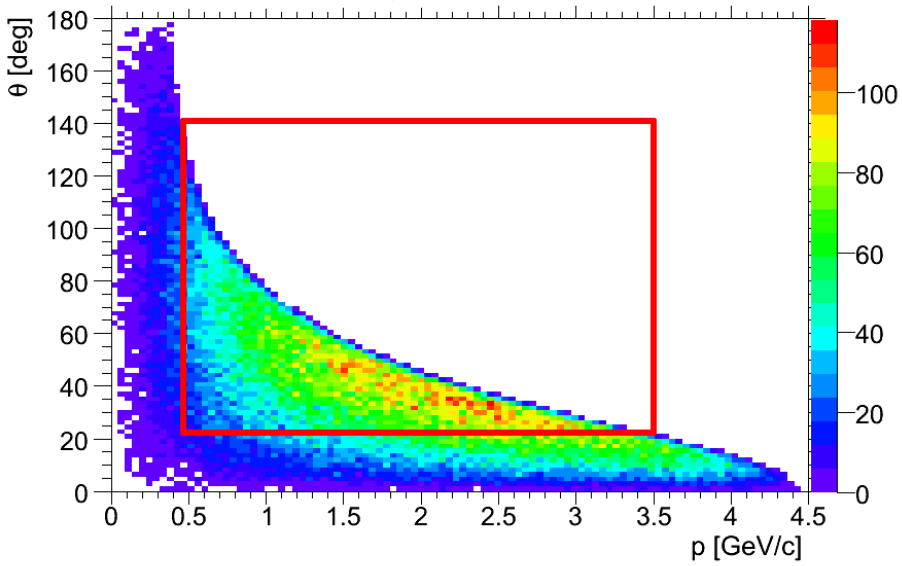

Figure 1. Intensity of kaons from $J/\psi \to K^+K^-\gamma$ from antiproton proton annihilations at $\sqrt{s} = 3.1$ GeV/c as function of polar angle θ and momentum p. The rectangle denotes the acceptance of the Barrel DIRC.

made of highly-polished synthetic fused silica with a refractive index of $n = 1.473$ at a wavelength of $\lambda = 380\,\text{nm}$. For $\beta \approx 1$ some of the photons will be caught inside the radiator due to total internal reflections and thus propagate towards the ends. Opposite surfaces are parallel. Thus the magnitude of the Cherenkov angle is preserved. One end is equipped with a mirror which reflects the photons towards the photon detectors where the angle of the photon is determined from the position measurement after traveling through an expansion volume (EV). The particle track information as obtained from a tracking system allows to reconstruct the track Cherenkov angle and to determine the corresponding PID likelihoods. The measured arrival time of the photon at the photon detector improves the resolution of the track Cherenkov angle. A good timing helps to disentangle events, a very good timing helps to get rid of reconstruction ambiguities, and an excellent timing could eliminate chromatic effects.

2 Baseline Design

The PANDA Barrel DIRC design is inspired by the successful BaBar DIRC counter [5]. Some key improvements are made to optimize the performance for PANDA. Focusing optics is used to improve the spatial resolution and to keep the small expansion volume inside the solenoid of the target-spectrometer. This allows to use shorter radiator bars and to simplify the overall detector integration. In addition, the smaller expansion volume decreases the sensitivity to accelerator-induced background. The fast timing helps to reconstruct Cherenkov cone angles and to clean up events from background.

The schematic view of the PANDA Barrel DIRC design is shown in figure 2. The radiators are narrow bars with the dimension $17 \times 53 \times 2400\,\text{mm}^3$. They are made by gluing two 1200 mm-long

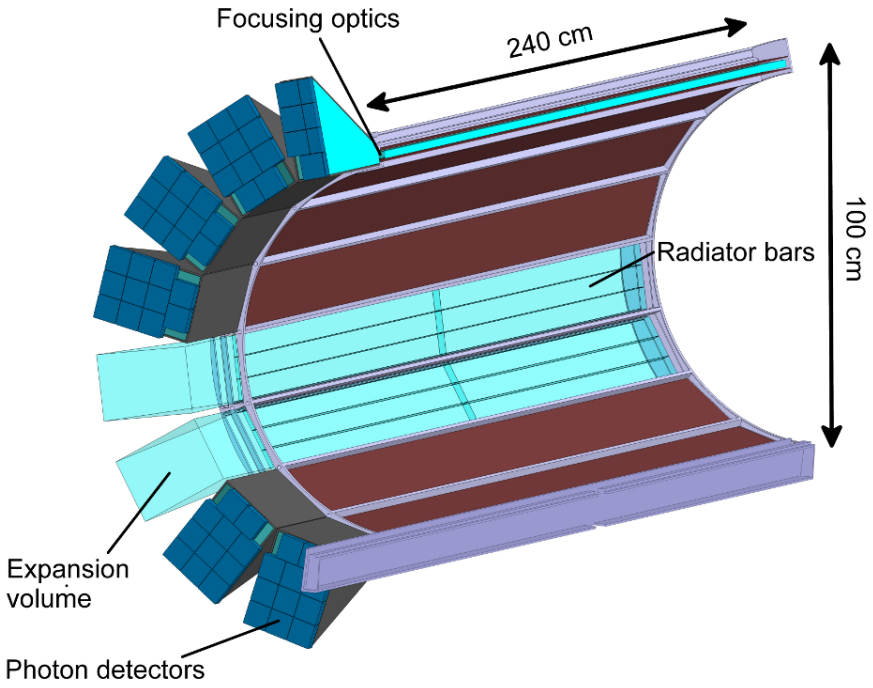

Figure 2. Schematic view of the PANDA Barrel DIRC design.

pieces back-to-back. In this figure, three bars are included in a bar-box, and 16 bar-boxes are each coupled optically to a prism as expansion volume with focusing lenses at the end of each bar. The lenses are made by interfacing the fused silica to high-refractive optical glass LaK33B avoiding air gaps. This is discussed in more detail in section 6. The longer face of the prism is equipped with position-sensitive photon detectors with about 11000 pixels. From the hit position and the direction of the charged particle, the Cherenkov angle of the photon can be deduced. The information about the direction of the charged particle comes from the tracking system. The photon detectors and the read-out electronics nearby have to work in the PANDA magnetic field, which has the strength of $B \approx 1\,\mathrm{T}$ in the region close to the magnetic end-cap of the solenoid. Microchannel-Plate PMTs (MCP-PMT) with multi-pixel readout fulfill these requirements and offer a good timing resolution. The aim for the whole electronic chain is to have a timing resolution of $\sigma \approx 100\,\mathrm{ps}$. The mechanical design is a modular concept. The expansion volume, together with the electronics, can be detached from the barrel holding the bar boxes with the radiators. This allows access to other detector systems within the barrel. The single bar boxes can be installed or removed with the help of rails from the barrel-shaped carbon fiber support structure.

The track Cherenkov angle resolution σ_{θ_C} is used to quantify the quality of the design. It is calculated from the quadratic sum of the single photon Cherenkov angle resolution (SPR) divided by the number of detected photons N_γ and the uncertainty of the charged particle track direction $\sigma^2_{\theta_C} = \mathrm{SPR}^2/N_\gamma + \sigma^2_{\mathrm{track}}$, which is dominated by multiple scattering and the resolution of the tracking detectors. The squared single photon resolution is the sum of the squared resolutions from the detector pixel size, the optical aberration and imaging errors, geometrical bar imperfections, and chromatic uncertainties due to dispersion. The expected SPR of the Barrel DIRC baseline

2016 JINST 11 C05013

design is 8–9 mrad, dominated by a 6 mrad contribution from the pixel size and about 5 mrad from chromatic dispersion. The dispersion can be partially corrected by precision timing at the level of 100 ps [6]. Between 15 and 60 detected Cherenkov photons are expected for a $\beta \approx 1$ particle, depending on the track angle. The π/K separation power can be calculated as $\Delta(\theta_C)/\sigma_{\theta_C}$, where $\Delta(\theta_C)$ is the difference of the expected Cherenkov angle for pions and kaons. At 3.5 GeV/c this angular difference is $\Delta(\theta_C) = 8.5$ mrad. Due to the asymmetric interactions in PANDA, the highest kaon track momenta are observed in the forward direction (figure 1). This is a good match to the performance of a Barrel DIRC, which is best for steep forward and backward angles where the photon yield is highest.

3 Design Options

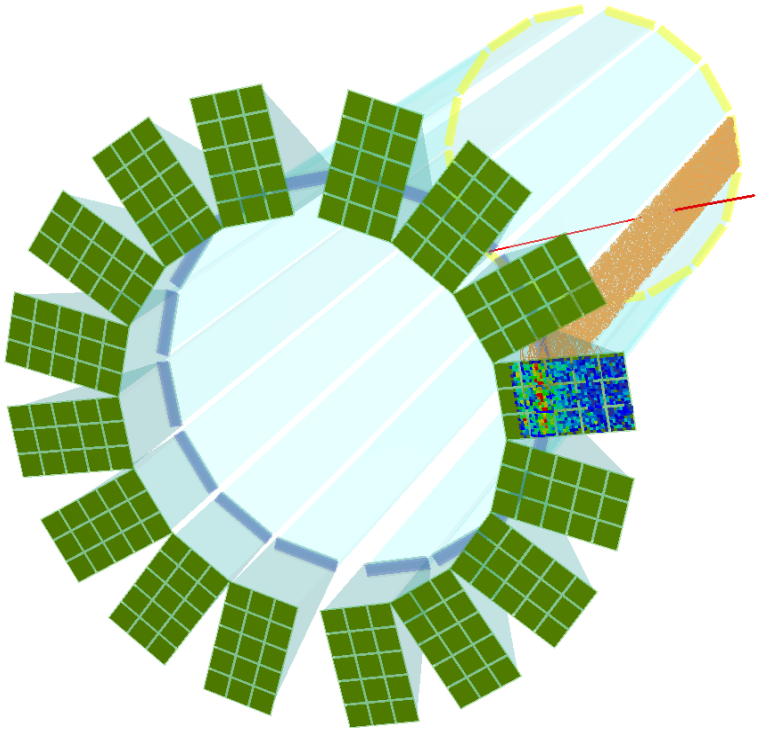

Figure 3. Geant simulation example of a PANDA Barrel DIRC design option with one wide radiator plate per bar box and prisms with a large opening angle and 15 MCP-PMTs per prism. The red line is a charged track producing photons (orange) in the radiator plate which are observed by the photon detectors (accumulated pattern from 100 kaons shown).

The initial PANDA Barrel DIRC design was guided by the successful BaBar DIRC detector [5], which achieved excellent π/K separation up to 4.2 GeV/c. This rather conservative approach used the same cross section for the radiator bars but a smaller expansion volume inside of the magnetic field. Due to the shorter expansion distance the pinhole focusing method, used by the BaBar DIRC counter, was not an option since the size of the bar and pixels could no longer be neglected compared to the expansion distance. Lenses or mirrors were needed as focusing elements to sharpen

2016 JINST 11 C05013

the Cherenkov ring image and the space limitations within the PANDA detector favor lenses. The focusing of photons onto the sensor plane can be facilitated with the use of complex spherical or cylindrical lens multiplet systems placed between the radiator and the expansion volume.

In the process of optimizing the design of the PANDA Barrel DIRC for cost and performance many different design aspects were investigated. These include the thickness and width of the radiators, the number of bars per sector, the material and shape of the focusing lenses, the material, shape, and size of the expansion volume, and the sensor layout on the focal plane [7].

Replacing the common expansion volume filled with mineral oil by 16 synthetic fused silica prisms coupled to 16 bar boxes has a twofold advantage: the read-out plane can become smaller and fewer MCP-PMTs are needed. Also, the superior optical quality of the fused silica results in a higher photon yield and the risk of spills of mineral oil is avoided. However, one has to consider that the additional reflections of photons at the sides of each prism complicate the observed Cherenkov pattern and the reconstruction of the Cherenkov angle.

The design option with the largest impact on the system cost is the number of bars within a bar box. The example of a bar box with the option of one wide plate and one prism per bar box is shown in figure 3. The use of a wide plate would result in a significant reduction of the radiator fabrication cost since fewer pieces have to be produced. The Belle II TOP detector has demonstrated that high-quality wide plates can be fabricated by optical industry [8]. However, a wide plate needs a different type of lens (or may require no focusing) and the PID algorithm requires a different approach compared to narrow bars. Both have to be studied in simulation and validated with experimental data.

Ultimately, the design optimization process resulted in the baseline design with 53 mm-wide bars and the potentially cost-saving design option with 160 mm-wide plates.

4 Simulation

In order to optimize the performance and to reduce the detector costs, realistic simulations of different design options were performed using Geant [9]. All detector components are assembled as Geant volumes and used as media for the particle transport. Figure 4 shows the side view of a bar box of the PANDA Barrel DIRC with the main parts and materials used in the simulation. These include the synthetic fused silica prism and bars, lenses made from fused silica and LaK33B [10] material, front-coated mirrors, as well as Epotek 301-2 glue and Eljen EJ-550 optical grease for connecting different components. The MCP-PMTs volumes comprise a fused silica entrance window and a bi-alkali photocathode. The mechanical structures are made of carbon-fiber-reinforced plastic (CFRP).

The simulation is performed within the PandaRoot framework [11]. It includes event generation, particle transport, digitization, hit finder and reconstruction. The particle transport uses the Virtual Monte Carlo approach, which allows for easy switch between Geant3 and Geant4 for systematic studies. The simulation of Cherenkov photons includes the wavelength-dependence of the transport efficiency inside of the bars and of the refractive indices of all materials. The digitization stage simulates the realistic detector response of the photon detectors. It includes charge sharing, dark noise, collection efficiency, geometric efficiency, quantum efficiency, and single photon timing resolution observed for the PHOTONIS Planacon MCP-PMTs [12].

2016 JINST 11 C05013

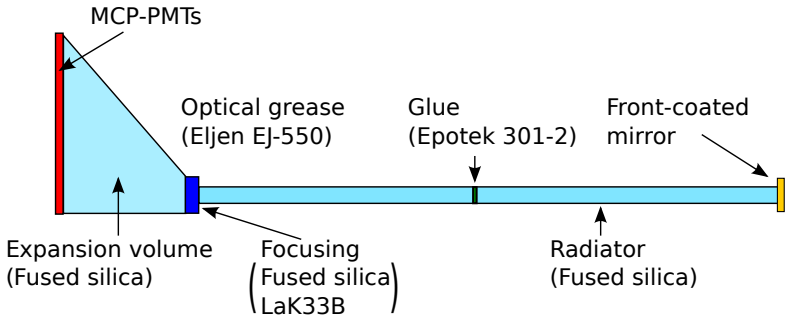

Figure 4. Schematic side view of the PANDA Barrel DIRC with the main components and their materials. Not to scale.

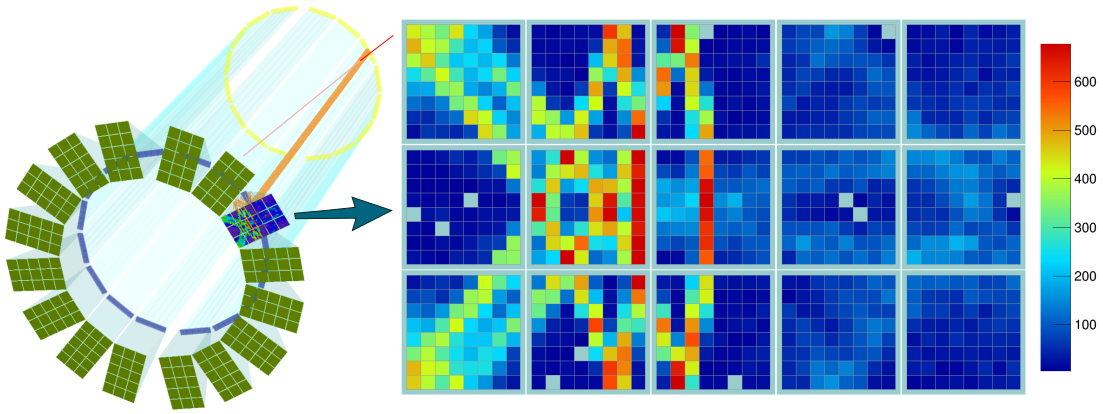

Figure 5. Geant simulation of the PANDA Barrel DIRC using narrow bars as radiators together with prism as expansion volume. The colored histogram shows the accumulated hit pattern from 1000 K^+ at 3.5 GeV/c and 25° polar angle.

Figure 5 shows the Geant representation of the PANDA Barrel DIRC geometry with the prism EV and the example of the hit pattern for 1000 K^+ at the same momentum and angle of incidence. In order to represent the real structure of the data output from the detector a time-based simulation has been implemented. The time-based data structure introduces additional challenges to the data processing. One such challenge is related to the possible loss of hits due to the pile-up of events and the dead time of the read-out. Figure 6 (a) shows the map of the loss rate as a function of dead time and event rate. The photon detectors together with the DAQ system, which is currently planned for the Barrel DIRC, have a dead time of about 40 ns. Together with the designed event rate for the PANDA experiment of 20 MHz, this yields a hit loss rate of about 5%.

Another challenge of the time-based structure of the data is an ambiguous assignment of hits to the events and particles. Due to the pile-up, the reconstructed event could contain hits from neighboring events (see figure 6 (b)). However, the tracks from different events usually hit different Barrel DIRC radiators and, therefore, produce hits which are well separated in space and can be successfully assigned to the corresponding events. According to the DPM [13] event generator simulation only 4% of events create tracks which pass through the same radiator. The hits from such events still can be correctly assigned in 90% of the cases based on the photon propagation time in the radiator.

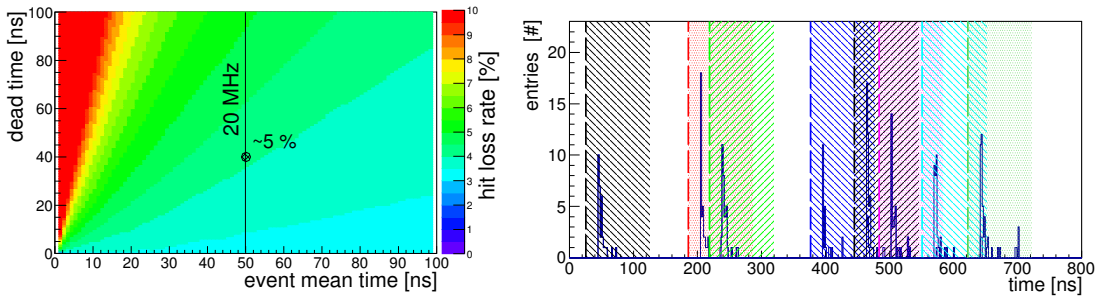

Figure 6. (a) Map of the hit loss rate due to the pile-up of events. The color scale indicates the percentage of lost hits. (b) Time spectrum of the hits after hit finder. Different colors represent different events. The vertical lines indicate the start time of the events. Shaded areas indicate the time window of a given reconstructed event.

5 Reconstruction

Two different reconstruction approaches have been developed to evaluate the detector resolution and performance of the various design options.

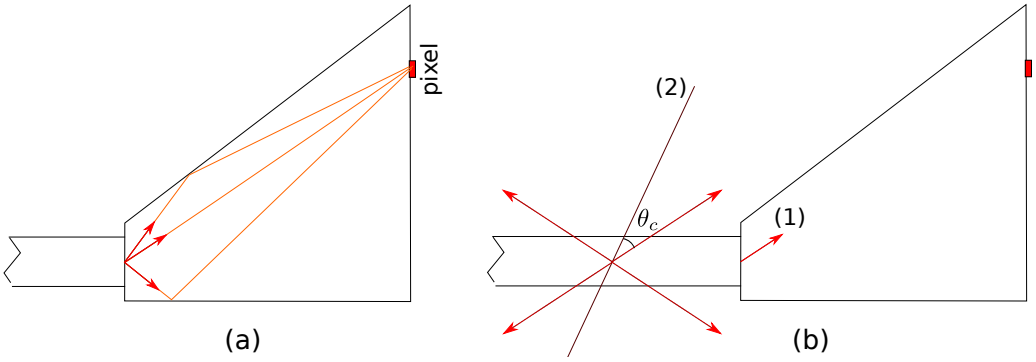

Figure 7. Schematic of the geometrical reconstruction method. (a) Different photon paths in the prism EV hitting the same pixel are stored in the LUT. (b) Determining the Cherenkov angle by calculating the angle between the photon direction from the LUT (1) and the charge track direction (2). Eight different combinations are possible (four are shown), which leads to combinatorial background.

The geometrical reconstruction method is based on look-up tables (LUTs) and was also used for the BaBar DIRC [5]. In this approach the direction of a detected photon is approximated by the three-dimensional vector between the center of the bar and the hit photon detector pixel. LUTs are produced from the full simulation using a photon gun to store, for each detector pixel, the direction vectors at the end of the bar for all photons that hit a given pixel (see figure 7 (a)). Those direction vectors are then combined with the particle momentum vector available from the tracking system to determine the photon Cherenkov angle θ_C (see figure 7 (b)). Each direction from the LUT needs to be combined with the particle direction in 8 different ways to account for all possible reflection from the sides of the bar. Together with different photon paths in the expansion volume they add ambiguous angles which, however, are mostly randomly distributed while the true combinations

2016 JINST 11 C05013

are always near the expected Cherenkov angle. Figure 8 (a) shows the reconstructed angles for one K^+ at 3.5 GeV/c which produced 52 measured Cherenkov photons. The mean value of the Gaussian peak in the distribution indicates the most probable θ_C. A reduction of the combinatorial background is achieved by applying a selection on the difference between the arrival time of the measured photon and the expected time. The latter is calculated based on the photon direction from the LUT assuming an average wavelength. Figure 8 (b) shows the time difference distribution for 100 K^+ at 3.5 GeV/c momentum and 25 degree polar angle. The asymmetric shoulder in the distribution is caused by path ambiguities inside the prism.

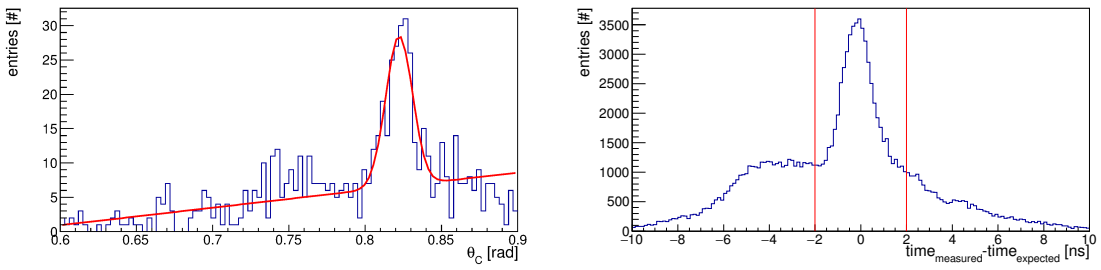

(a) **(b)**

Figure 8. (a) Example of the single photon Cherenkov angle resolution (SPR) for a single K^+ track with 3.5 GeV/c momentum emitted at an polar angle of 25°. The fit determines a SPR of about 9 mrad. (b) Time difference between measured and expected arrival times of the Cherenkov photons from 100 K^+. The vertical lines indicate the selection region.

The performance of the detector design is evaluated in terms of the reconstructed single photon Cherenkov angle resolution (SPR) and the photon yield per particle. The SPR is defined as the difference of the expected and the reconstructed Cherenkov angle for the individual photons.

The performance of the design configurations with narrow bars, together with different EV and focusing has been described in ref. [2, 14]. It was shown that the configuration with a spherical lens without air gap as a focusing system satisfies the PANDA Barrel DIRC requirements. Additional studies were performed to optimize the design in terms of costs. A significant reduction of the costs is expected by reducing the number of fused silica bars in each bar box. Using three 53 mm wide bars instead of five 32 mm wide bars gives the same azimuthal geometrical coverage. Figure 9 shows the comparison of the photon yield and the SPR for five and three bars in a bar box. It is worth noting that the thickness of the focusing lens system increases for wider bars leading to a small increase in photon loss due to reflections inside the lens.

The number of Cherenkov photons ranges from 15 to 60 for the geometry with 3 bars, which is about 10% lower than for the design with 5 bars. The loss of photons happens inside the lenses of the focusing system, which is assumed to have non-reflective sides. Both distributions have a peak near perpendicular incidence at 90° where the entire Cherenkov cone is totally internally reflected. The yield drops as part of the ring escapes the bar and it rises again as the length of the track in the bar increases. The SPR for both configurations is about the same and lies within the range of 8–11 mrad, depending on the polar angle of the track.

Figure 10 shows the track Cherenkov angle resolution σ_{θ_C} for the design with three bars, a

2016 JINST 11 C05013

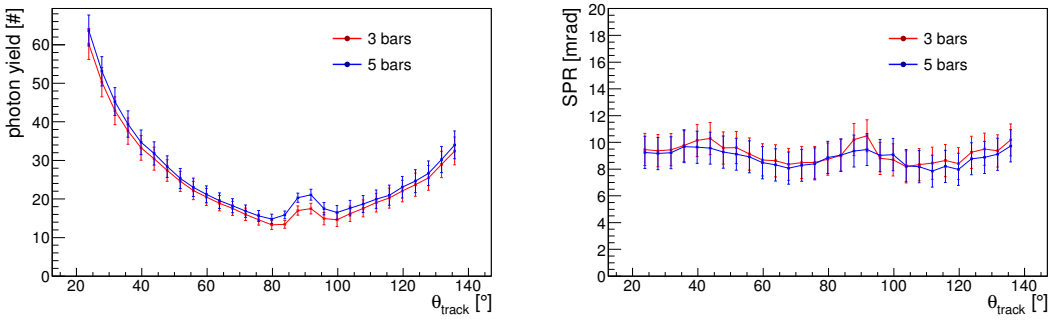

(a) **(b)**

Figure 9. Photon yield (a) and SPR (b) for a prism-type EV with 3 bars (red) and 5 bars (blue) radiator box for kaons with 3.5 GeV/c momentum. The error bars correspond to the rms of the distributions in each bin.

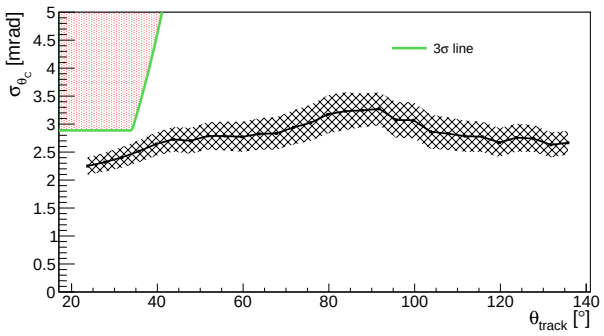

Figure 10. Track Cherenkov angle resolution for 3.5 GeV/c kaons as a function of the polar angle for a design with 53 mm wide bars, fused silica prism EV, and a spherical lens.

fused silica prism EV, and a spherical lens as a function of the particle polar angle. A tracking resolution of $\sigma_{\text{track}} = 1.7$–$2.3$ mrad, depending on the polar angle, is included. The green curve corresponds to the track Cherenkov angle resolution value corresponding to exactly 3 s.d. π/K separation at the highest momentum. The green curve flattens out below 35° for the maximum momentum of 3.5 GeV/c due to the momentum/polar angle correlation in PANDA (see figure 1). All σ_{θ_C} values below the green curve meet the PID requirements in PANDA. The track Cherenkov angle resolution of 1.8–2.9 mrad for this design is better than the required resolution for the entire polar angle range and thus meets the PID requirements for PANDA.

The geometrical reconstruction approach is not suitable for wide plates since the assumption that the photons exit from the center of the radiator is no longer a good one. An alternative time-based imaging method was developed, similar to the approach used by the Belle II Time-Of-Propagation counter [15]. For each pixel, the full simulation is used to record the arrival time of photons from e, μ, π, K, p, which are then stored in an array of normalized histograms to produce probability density functions (PDF). An example for one MCP-PMT pixel is shown in figure 11 (a). The resolution of the detected time was assumed to be 100 ps in simulation, the expected single photon timing resolution in PANDA.

For a given track the observed photon arrival time for each pixel with a hit is compared to the

2016 JINST 11 C05013

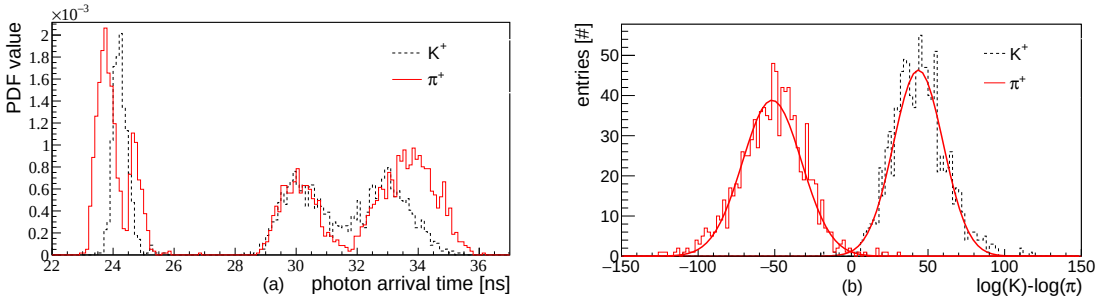

Figure 11. Examples for the time-based reconstruction of the plate geometry with a prism EV and without focusing: photon arrival time for charged pions and kaons for a selected MCP-PMT pixel (a) and log-likelihood difference for kaon and pion hypotheses for a sample of 3.5 GeV/c pions and kaons at 22° polar angle (b).

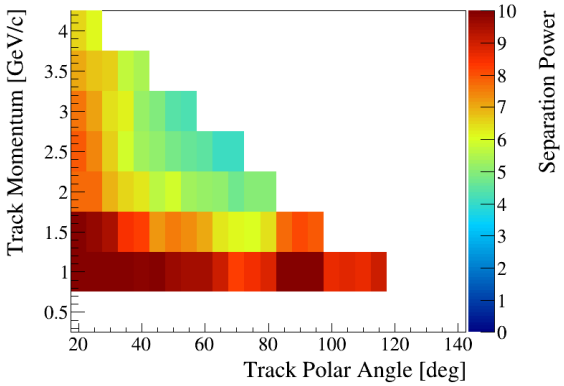

Figure 12. Separation power of kaons and pions for a wide plate and a prism EV without focusing as result of time-based imaging reconstruction for a single photon time resolution of 100 ps.

histogram array to calculate the time-based likelihood for the photons to originate from a given particle hypothesis. Combining this likelihood with the Poissonian PDF of the number of observed photons creates the full likelihood. Figure 11 (b) shows the log-likelihood difference for kaon and pion hypotheses for a sample of 3.5 GeV/c pions and kaons at 22° polar angle. The corresponding π/K separation, calculated as the difference of the two mean values of the fitted Gaussians divided by the average width, corresponds to about 5.1 s.d. A detailed study was carried out on many points of the Barrel DIRC phase-space acceptance region. Figure 12 shows the results without focusing. All points in the diagram meet or exceed the required π/K separation.

6 Prototyping

The simulated design options have been validated in particle beams. This is accompanied by laboratory measurements of component prototypes on test benches, using electronic pulsers and lasers. Examples are photon detectors, readout electronics, optical lenses, and radiators from different manufacturers.

2016 JINST 11 C05013

The detection of single photons with good resolution, 100 ps or better in time and few mm in space, is one of the technical challenges for the PANDA Barrel DIRC. In addition, the photon detector has to work in a 1 T magnetic field and has to withstand event rates of up to 20 MHz. The choice are MCP-PMTs with increased lifetime. Two models, PHOTONIS Planacon XP85112 and Hamamatsu R13266-07-64 have been identified [12] which meet all Barrel DIRC sensor specifications. These detectors are read out by a data acquisition system based on the trigger and readout board (TRB3) and the PADIWA discriminator card [16].

The optical and mechanical quality of the DIRC radiators are of critical importance for the photon yield and the single photon resolution. Depending on the particle polar angle Cherenkov photons are internally reflected up to 200 times before exiting the bar. The probability of photon loss due to total internal reflection is determined by the surface roughness and sub-surface damage, created in the fabrication process. A transport efficiency of 90% requires a surface polish at the level of 5-10 Å. To maintain the magnitude of the Cherenkov angle during the reflections the bar surfaces have to be parallel and square within 0.25 mrad. During the PANDA Barrel DIRC prototyping program a total of about 30 bars and plates were produced by seven manufacturers, using different materials and fabrication techniques. The quality of these prototypes has been tested in three separate experimental setups. Two setups measure the parallelism and squareness of the bar surfaces. One uses an autocollimator and the other a laser reflected from the bar sides. The angular precision achieved is better than 0.1 mrad. Bars from several of the manufacturers were found to meet the angular specifications. Another setup determines the coefficient of total internal reflection. The fraction of light transmitted after about 50 internal reflections in a bar is measured using several laser wavelengths and is related to a surface roughness of about 5 Å via the scalar scattering theory [17].

The development of an optical lens with a focal plane matching the photon detector surface and a high transmission probability for photons into the expansion volume is an important issue. Conventional optics employ glass/air interfaces for refraction. However, the transition from a focusing concave fused silica surface to air traps many photons with shallow incident angles by internal reflection in the fused silica. Therefore, a lens with a refractive index larger than fused silica was chosen. An early version used a single focusing surface and is described in reference [2]. Another lens design uses two refracting surfaces to achieve a flat focal plane. Figure 13 (left) shows the three components: the two fused silica parts are for the coupling of the lens to the radiator bar and the expansion volume. The middle part is made from lanthanum crown glass (LaK33B) and has two surfaces with different curvatures, one defocusing surface on the side coupled to the bar and a focusing surface on the prism-side. The LaK33B material was chosen due to the high refractive index of n= 1.786 and a good transmission of T= 0.954 for a 10 mm thick sample at a wavelength of λ = 380 nm. The lens was designed with the Zemax optical software [18]. The prediction of this software package was cross-checked with the Geant simulation package. The results are shown in figure 13 (right).

A prototype of such a high-refractive index compound lens has been built by a glass company [19] and tested in a Barrel DIRC prototype (figure 14) as described below. Since radiation hardness of the lanthanum crown glass in the PANDA environment is a concern, other high-refractive index materials are being studied and the radiation hardness of the lens prototype is being tested [20].

2016 JINST 11 C05013

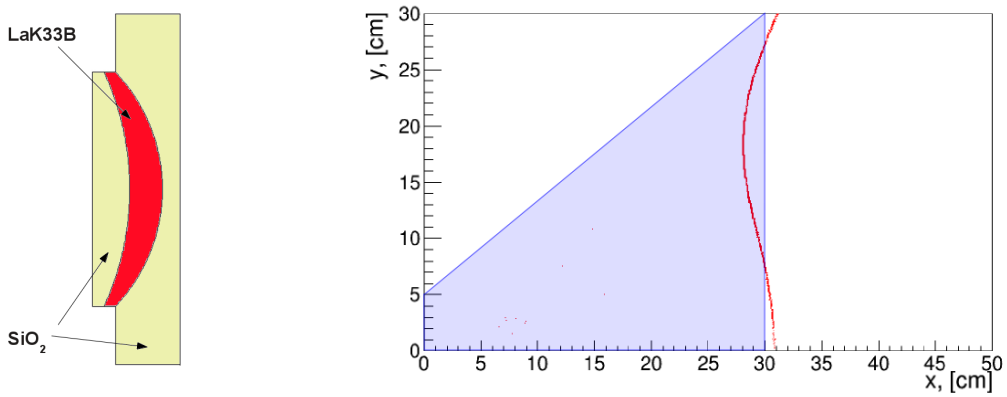

Figure 13. Schematic of the spherical three-component lens (left) and the focal plane as red curve simulated by the Geant4 software package (right). The blue shaded area depicts the expansion volume.

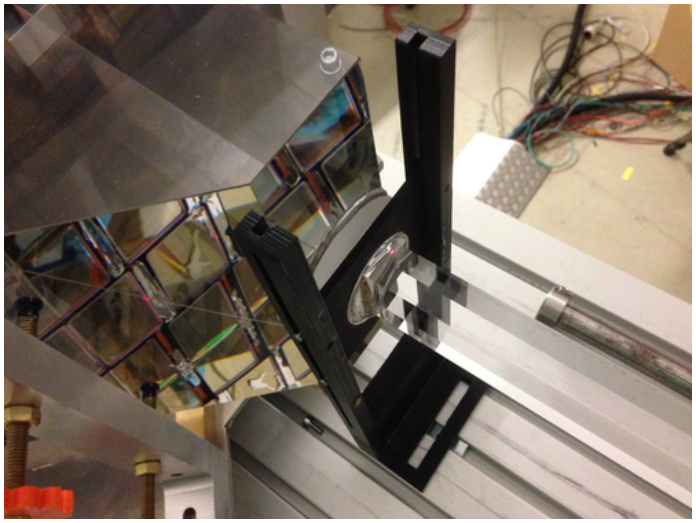

Figure 14. The lens prototype between the expansion prism and the radiator.

Three system prototypes were tested in particle beams at GSI and CERN from 2011–2015. They all feature a dark box containing a radiator bar coupled to an expansion volume, equipped at the back side with a photon detector array read out by a TRB system [2]. In the summer of 2015 a fourth prototype was tested in a charged mixed particle beam at CERN [20]. Within 34 days some 500 million events were recorded and a multitude of configurations were tested. A bar and a plate with spherical and cylindrical lenses with high refractive index were used, and a wide range of beam-bar angles and positions were tested. The particle beam hit the radiator bar of the prototype setup shown in figure 15. The polar angle between the radiator and the beam was adjustable and verified using a remotely operated motor and a camera. The vertical and horizontal position of the beam on the radiator could be changed by hand and checked with gauges. Two scintillation counters ("Trigger 1" and "Trigger 2" in figure 15) triggered the readout electronics. Two PHOTONIS Planacon MCP-PMTs were placed in the beamline, separated by a distance of 29 m ("TOF 1" and "TOF 2"), to separate protons from pions and electrons by measuring their time of flight.

2016 JINST 11 C05013

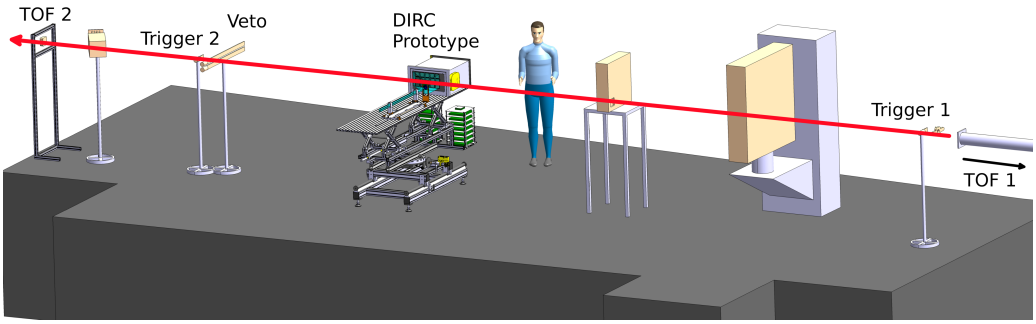

Figure 15. Schematic view of the prototype configuration at CERN-T9 in 2015.

An array of 3×5 MCP-PMTs (PHOTONIS XP85012) with 960 pixels was read out by PADIWA discriminator cards. The discriminating thresholds for the MCP-PMT signals were individually adjusted in the sub-millivolt range. The TRB system recorded the time difference between the trigger signal and the discriminator signals. Noise events and other spurious contributions, e.g. photons from delta electrons in the radiator bar were cut out by this timing information. Electronic channels with a high background count-rate were masked. Due to different timing offsets of the individual electronic channels, calibration runs with laser pulses with picosecond accuracy were taken and the data corrected accordingly. The TOF counters were used to cleanly select protons with a separation power of about 6 s.d. at a momentum of $p = 7$ GeV/c.

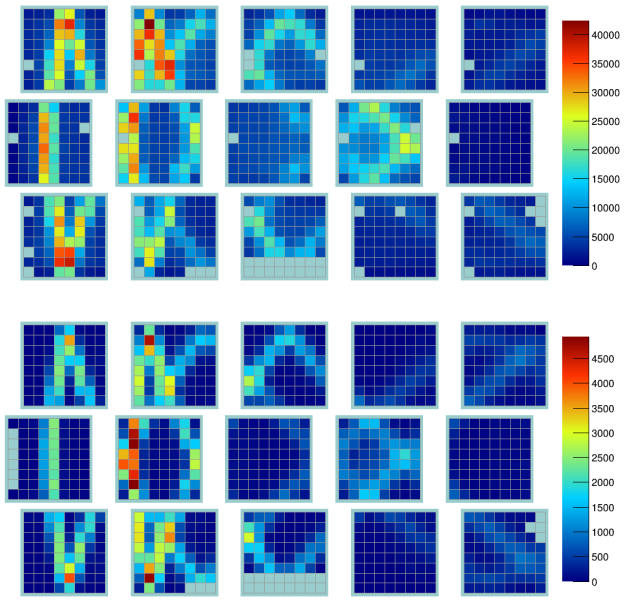

Figure 16. Array of 3×5 Planacon MCP-PMTs with 960 pixels with a Cherenkov pattern from $p = 7$ GeV/c protons in data (top) and simulation (bottom).

After having processed the data in this way, the experimentally observed Cherenkov ring image in figure 16 (top) can be compared to the simulation in figure 16 (bottom). The pattern is a Cherenkov ring folded by reflections in the radiator and in the prism and the experimental distribution in well-described by simulation.

2016 JINST 11 C05013

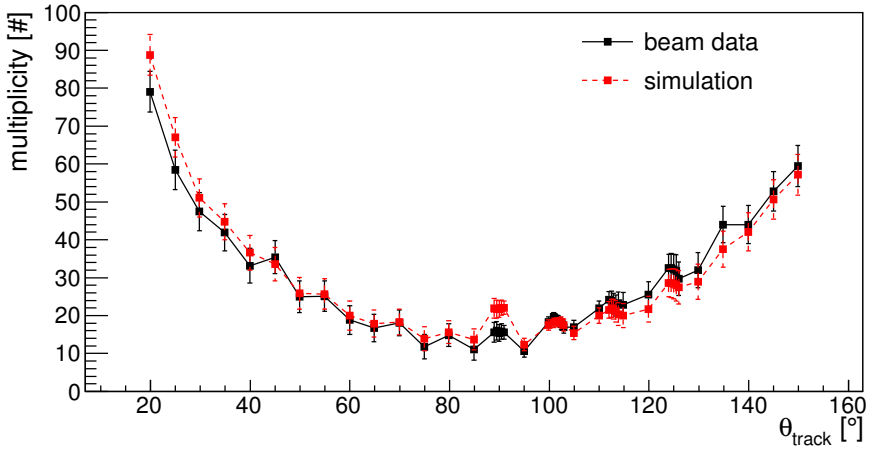

Figure 17. Photon yield as function of the track polar angle for $p = 7$ GeV/c protons in data and simulation as black and red symbols, respectively. The error bars correspond to the rms distribution in each bin.

The photon yield as a function of the track polar angle is shown in figure 17. The black symbols denote the data and the red symbols the simulation results. The simulation results include contributions from δ electrons and from charge sharing between MCP-PMT anode pads. The agreement between data and simulation is generally within the fluctuations of the data points. For forward angles $\theta < 40°$ and for near-perpendicular incidence the simulation overestimates the photon yield. A possible explanation may be that the optical properties of the mirror, which affects only photons from tracks with polar angles smaller than 95°, are not simulated correctly. This deviation is currently under study and needs further analysis.

The single photon angle Cherenkov resolution for the same data set is shown in figure 18. While for small and large track polar angles the data and simulation agree within the statistical fluctuations,

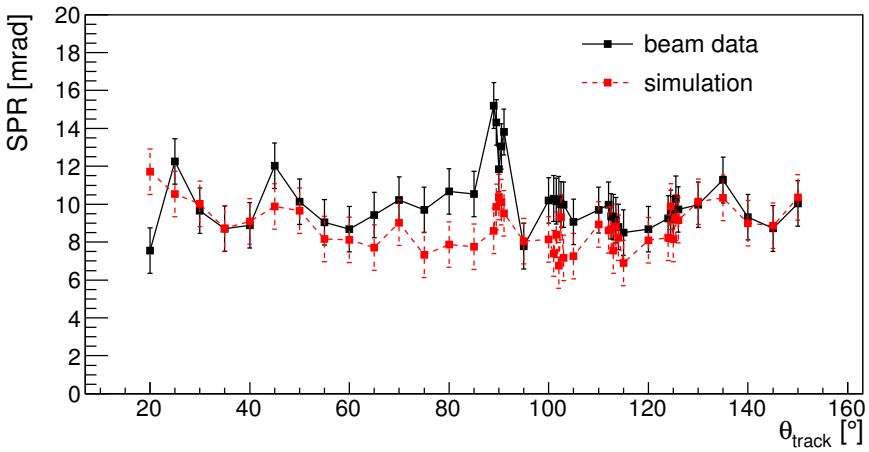

Figure 18. Single photon angle resolution (SPR) as function of the track polar angle for $p = 7$ GeV/c protons in data and simulation as black and red symbols, respectively. The error bars correspond to the rms distribution in each bin.

2016 JINST 11 C05013

the angles around $\theta \approx 90^\circ$ show a resolution 2–3 mrad worse than predicted. In this angular range, geometrical ambiguities play an important role for the reconstruction and the deviation between data and simulation need to be further investigated. However, it is important to note that, due to the large Cherenkov angle difference for particles observed in PANDA at these polar angles, the SPR degradation observed has no significant impact on the PID performance of the narrow bar design.

The experimental data obtained with the wide plate showed a good qualitative agreement of the Cherenkov hit patterns with simulation in both the pixel space and the photon hit time space. However, since the time resolution obtained during the beam test was a factor of 2–3 worse than the required resolution of 100 ps per photon, another prototype test with improved timing is scheduled at the CERN PS for October 2016 to validate the PID performance of the cost-saving design with wide plates.

7 Conclusion

Important design elements of the PANDA Barrel DIRC have been studied using simulation and system prototypes with particle beams. The single photon yield, the single photon Cherenkov angle resolution, and the predicted PID performance were evaluated for many design options using a geometric reconstruction method for narrow radiator bars and a time-based likelihood approach for wide radiator plates.

The baseline design was validated using a prototype with a narrow bar, a three-component spherical lens, and a fused silica prism in a beam test at CERN. The performance parameters were found to be in good agreement with simulation and to meet or exceed the PID requirement of three standard deviations π/K separation up to a track momentum of 3.5 GeV/c within the acceptance of the PANDA Barrel DIRC.

While the time resolution obtained during the 2015 beam test was not sufficiently good to validate the PID performance of the wide radiator plate, the potential cost savings and simplification of this design warrant another beam test with improved readout electronics, scheduled for the fall of 2016.

These results will form the basis for the Technical Design Report, expected to be completed by the end of 2016.

Acknowledgments

This work was supported by HGS-HIRe, HIC for FAIR, EU FP7 grant #227431, BNL eRD4, U.S. National Science Foundation PHY-125782., and BMBF contract number 05E12CD2. We thank the GSI and CERN staff for the opportunity to use the beam facilities and for their on-site support.

References

[1] PANDA collaboration, M.F.M. Lutz et al., *Physics Performance Report for PANDA: Strong Interaction Studies with Antiprotons*, arXiv:0903.3905.

[2] PANDA Cherenkov Group, M. Hoek et al., *The PANDA Barrel DIRC detector*, *Nucl. Instrum. Meth.* **A 766** (2014) 9.

2016 JINST 11 C05013

[3] PANDA Cherenkov Group, E. Etzelmüller et al., *The PANDA Disc DIRC Project at FAIR*, in *International Workshop on Fast Cherenkov Detectors - Photon detection, DIRC design and DAQ*, November 11–13, 2015, Giessen, Germany.

[4] PANDA Cherenkov Group, K. Beloborodov et al., *The Forward RICH Project at PANDA*, in *International Workshop on Fast Cherenkov Detectors - Photon detection, DIRC design and DAQ*, November 11–13, 2015, Giessen, Germany.

[5] BaBar DIRC collaboration, I. Adam et al., *The DIRC particle identification system for the BaBar experiment*, *Nucl. Instrum. Meth.* **A 538** (2005) 281.

[6] J. Benitez, D.W. G.S. Leith, G. Mazaheri, B.N. Ratcliff, J. Schwiening, J. Vavra et al., *Status of the Fast Focusing DIRC (fDIRC)*, *Nucl. Instrum. Meth.* **A 595** (2008) 104.

[7] M. Patsyuk, *Simulation, Reconstruction and Design Optimization for the PANDA Barrel DIRC*, PhD thesis, Goethe-Universität Frankfurt am Main (2015).

[8] BELLE II PID collaboration, P. Krisan, *Particle identification at Belle II*, 2014 *JINST* **9** C07018.

[9] GEANT4 collaboration, S. Agostinelli et al., *GEANT4: A Simulation toolkit*, *Nucl. Instrum. Meth.* **A 506** (2003) 250;
J. Allison et al., *Geant4 developments and applications*, *IEEE Trans. Nucl. Sci.* **53** (2006) 270.

[10] Optical Glass Data Sheets, Schott AG, 25.04.2013.

[11] PANDA collaboration, S. Spataro, *Simulation and event reconstruction inside the PandaRoot framework*, *J. Phys. Conf. Ser.* **119** (2008) 032035;
M. Al-Turany and F. Uhlig, *FairRoot Framework*, PoS(ACAT08)048.

[12] A. Lehmann et al., *Lifetime of MCP-PMTs*, in *International Workshop on Fast Cherenkov Detectors - Photon detection, DIRC design and DAQ*, November 11–13, 2015, Giessen, Germany.

[13] A. Capella, U. Sukhatme, C.-I. Tan and J. Tran Thanh Van, *Dual parton model*, *Phys. Rept.* **236** (1994) 225.

[14] PANDA Cherenkov Group, R. Dzhygadlo et al., *Simulation and reconstruction of the PANDA Barrel DIRC*, *Nucl. Instrum. Meth.* **A 766** (2014) 263.

[15] M. Staric, *Pattern recognition for the time-of-propagation counter*, *Nucl. Instrum. Meth.* **A 639** (2011) 252.

[16] M. Traxler et al., *TRB development*, in *International Workshop on Fast Cherenkov Detectors - Photon detection, DIRC design and DAQ*, November 11–13, 2015, Giessen, Germany.

[17] J. Elson, H. Bennet and J. Bennet, *Scattering from Optical Surfaces*, in *Applied Optics and Optical Engeneering Vol. VII*, Chapter 7, Academic Press (1979).

[18] Zemax Europe, 8 Riverside Business Park, Stoney Common Road, Stansted CM24 8PL, United Kingdom, http://www.zemax.com.

[19] Befort Wetzlar OD GmbH, Braunfelser Str. 26-30, 35578 Wetzlar, Germany, http://www.befort-optic.com.

[20] G. Kalizy et al., *DIRC detector for the future Electron Ion Collider experiment*, in *International Workshop on Fast Cherenkov Detectors - Photon detection, DIRC design and DAQ*, November 11–13, 2015, Giessen, Germany.

2016 JINST 11 C05013